Contents lists available at ScienceDirect

Sensors and Actuators B: Chemical

journal homepage: www.elsevier.com/locate/snb

Highly sensitive volatile organic compounds vapour measurements using a long period grating optical fibre sensor coated with metal organic framework ZIF-8

Jiri Hromadka [a,b], Begum Tokay [c], Ricardo Correia [a], Stephen P. Morgan [a], Sergiy Korposh [a,*]

[a] Optics and Photonics Group, Faculty of Engineering, University of Nottingham, University Park, Nottingham NG7 2RD, United Kingdom
[b] Institute for Environmental Studies, Faculty of Sciences, Charles University in Prague, Benátská 2, CZ 12843 Praha 2, Czech Republic
[c] Chemical and Environmental Engineering Department, Faculty of Engineering, University of Nottingham, University Park, Nottingham NG7 2RD, United Kingdom

ARTICLE INFO

ABSTRACT

An optical fibre long period grating (LPG) based volatile organic compound (VOC) sensor coated with ZIF-8, a material from the zeolite imidazolate framework (ZIF) family, functional coating is presented. ZIF-8 film was deposited onto the surface of the LPG using an in-situ crystallization technique by mixing freshly prepared 12.5 mM zinc nitrate hexahydrate and 25 mM 2-metyl-imidazole solutions in methanol. A concentration specific response to acetone, ethanol and methanol vapour was obtained over the high concentration range up to tens thousands ppm. The LPG based sensor works at phase-matching turning point (PMTP) and such operates at the highest sensitivity. A novel approach for the data analysis based on the measurement of the bandwidth of the U-shaped attenuation band of the LPG is introduced. The optimized sensor shows a sensitivity of 0.015 ± 0.001 and 0.018 ± 0.0015 nm/ppm and limit of detection (LOD) of 6.67 and 5.56 ppm for acetone and ethanol respectively.

© 2018 The Authors. Published by Elsevier B.V. This is an open access article under the CC BY license (http://creativecommons.org/licenses/by/4.0/).

1. Introduction

The fabrication of low-cost, portable, accurate and real-time sensors for organic vapour detection is of considerable interest in biomedical fields and in food quality monitoring [1]. Ethanol and acetone represent the most common examples of volatile organic compounds (VOCs). The measurement of ethanol in breath is of high interest in traffic safety [2], where the accepted alcohol limits in blood vary across Europe from 0.2 to 0.8‰, which corresponds to a concentration of 30–130 ppm in breath [2]. The detection of acetone in breath is important in medical diagnostics, where the increase of acetone concentration (single ppm units) can be related to diabetes [3] and high concentration (tens-hundreds ppm) is observed as symptom of ketoacidosis [4]. VOCs are usually measured using gas chromatography–mass spectroscopy (GC–MS), however, the detection is expensive and needs experienced personnel [5]. Currently,

most ethanol sensors are based on metal oxide semiconductors such as SnO_2 [6], WO_3 [7], In_2O_3 [8], Fe_2O_3 [9] and ZnO [10]. Semiconducting material based sensors exhibit high sensitivity whilst they usually operate at high temperatures (200–400 °C) to achieve chemical reactivity between the sensing material and the target gases. Also the fabrication of the sensitive layer should be conducted at high temperature and thus is associated with high energy consumption [11,12].

Fibre-optic sensing platforms are small, lightweight, immune to electromagnetic interference and as such can be used in extreme conditions, enabling remote real time monitoring with no electrical power needed at the sensing point [13]. There have been a number of fibre-optic based ethanol gas sensors proposed recently using the deposition of the sensitive layer on the fibre tip to form Fabry-Perot interferometers [14–18] or evanescent wave sensors, where part of the cladding is mechanically or chemically removed and then the functional coating is deposited over the stripped region [11,19–22]. A coating sensitive to ethanol vapours has been also applied on the surface of a photonic crystal fibre [23], long period grating (LPG) [24] or quartz crystal microbalance (QCM). The properties of pub-

* Corresponding author.
E-mail address: s.korposh@nottingham.ac.uk (S. Korposh).

Table 1
Summary of ethanol gas fibre optic sensors (LOD – limit of detection).

Sensor type	Sensor principle	Coating	Tested range	Sensitivity	Resp. time	LOD	Ref.
Fabry–Perot interferometer (FPI)–film on the fibre tip	Δ of fibre-film reflectance	Single wall carbon nanotubes (SWCNT)	63 and 73 ppm	0.9×10^{-4}/ppm	~3 min*	n/a	[14]
FPI–film on the fibre tip	Δ of fibre-film reflectance	SWCNT + cadmium arachidate	63 and 73 ppm	5×10^{-4}/ppm	~3 min*	n/a	[14]
FPI–film on the fibre tip	Δ in fluorescence; two sensors tested	vapochromic complex $[Au_2Ag_2(C_6F_5)_4(C_6H_5N)_2]$	1747 ppm (one value only)	1 dB and 3 dB per 1747 ppm	36 s/~5 min	n/a	[15]
FPI–film on the fibre tip	Δ of fibre-film reflectance	vapochromic complex–2,2′-bipyridine + Liquicoat*	25–127 ppm	0.0242 dB/ppm	20 to 30 min	2.74 ppm	[16]
Extrinsic sensor	Δ in fluorescence of nicotinamide adenine dinucleotide (NADH)	alcohol dehydrogenase (ADH)	0.30–300 ppm	17.45 a.u./ppm	n/a	n/a	[25]
Long period grating (LPG); period of 407 μm	Δ in intensity of the attenuation band	ZnO nanorods	~ 50 Torr (saturated EtOH pressure)	~4.4 dB	~80 min	n/a	[24]
Cladding removed–poly-methyl methacrylate (PMMA) optical fibre	Δ in intensity at 678 nm	SWCNT	12.5–500 ppm	0.26 a.u./ppm	~90 min	n/a	[19]
FPI–film on the fibre tip	Δ in luminescence from the QDs at 750 nm	fluorescent silicon quantum dots (Si- QDs)	533–1305 ppm in dry O_2 atmosphere	n/a	~1 min	~380 ppm	[17]
Cladding removed PMMA optical fibre	Δ in intensity at selected wavelengths	Multi-wall carbon nanotubes (MWCN)	50–500 ppm	0.52 a.u./ppm (saturation at ~350 ppm)	n/a	n/a	[11]
Cladding removed PMMA optical fibre	Δ in intensity at selected wavelengths	Sm_2O_3	0 to 500 ppm	76×10^{-3} au/ppm	78 min	n/a	[20]
Cladding removed PMMA optical fibre	Δ in intensity at selected wavelengths	Graphene oxide	100 to 500 ppm	0.26 a.u./ppm	n/a	n/a	[21]
Cladding removed silica optical fibre	Δ in power at selected wavelength	SnO_2	1000 to 20,000 ppm	~0.02 μW/1000 ppm (Saturated at 15,000 ppm)	10–18 s	n/a	[22]
FPI–film on the fibre tip –PMMA fibre	Δ in intensity at selected wavelengths	ZnO nanorods	Saturated vapour	Δ10.53% in reflected intensity	n/a	n/a	[18]
Quartz crystal microbalance (QCM)	Δ frequency	organic polymer (pen- tacene)	3074–15374 ppm	~0.0064 Hz/ppm	~30 s	n/a	[26]
Photonic crystal	Δ Bragg diffraction peak λ	Poly-acrylate type	EtOH/water p/p_0 (0.2-1)	Max λ shift of 59 nm/pure EtOH gas	n/a	n/a	[23]

lished ethanol gas fibre optic based sensors (and one example of a QCM) are summarized in Table 1. Reported sensors suffer mostly from a high response time in a range of 10 s min [19,24] and are usually tested over a limited concentration range. For example, they are tested at saturated vapour conditions [18,24], high (in a range of thousands of ppm) [22,23,26] or low level concentrations usually below 500 ppm [11,14,19–21]. The comparison in sensitivity shown in Table 1 is limited as only two papers show the limit of detection of 2.74 [16] and 380 ppm [17].

Among the different types of fibre-optic sensors, those based on gratings, specifically LPGs, have been employed extensively for refractive index measurements [27] and for monitoring associated chemical processes [27], since they offer wavelength-encoded information which overcomes the referencing issues associated with intensity based approaches. A LPG consists of a periodic perturbation of the refractive index of the fibre core, which couples the core mode to the co-propagating cladding modes of the fibre. This coupling is manifested in the transmission spectrum of the optical fibre as a series of resonance bands. Each resonance band corresponds to coupling to a different cladding mode and thus shows different sensitivity to environmental changes [28]. The coupling wavelength can be obtained from the following phase matching equation

$$\lambda_x = (n_{core} - n_{clad(x)})\Lambda \qquad (1)$$

where λ_x represents the wavelength at which light is coupled to the LP_{0x} cladding mode, n_{core} is the effective refractive index of the mode propagating in the core of the fibre, $n_{clad(x)}$ is the effective index of the LP_{0x} cladding mode and Λ is the period of the LPG [28]. The central wavelength of the resonance band is sensitive to changes in the surrounding environment such as temperature or external index of refraction [28]. It has been shown that the phase matching condition for the higher order cladding modes contains a turning point and that the LPG exhibits the

highest sensitivity when phase matching turning point (PMTP) is reached. At PMTP the U-shaped attenuation band growth larger (i.e. transmission decreases) and then splits into two bands that move into opposite directions. Measurements of the wavelengths separation or width of the band, as will be shown in this work, allows to achieve higher sensitivity. This can be achieved by choosing an appropriate LPG period and coating thickness [29,30]. The cladding modes associated with the attenuation bands have been calculated through numerical modelling using the phase matching equation and weakly guided approximation to determine the effective refractive indices of the core and cladding modes and the known values of the central wavelengths and the grating period [31].

The key element of a LPG based chemical sensor is the sensitive layer that captures the analyte. It has been shown that metal organic frameworks (MOFs), because of their unique properties, such as high surface area, adjustable shape and size of the pores and inner cavities, offer an ideal platform for the development of this sensitive layer [32–34]. The sensing mechanism of the LPG towards VOCs is based on the change of the refractive index of the sensitive layer due to the analyte of interest. It is therefore important to select MOFs that provide a specific and sensitive change in refractive index. Among the variety of MOFs, a zeolitic imidazole framework (ZIF)–ZIF-8 possesses properties that show promise for sensor development, such as its chemical robustness and thermal stability due to the sodalite (SOD) type of structure. The structure of ZIF-8 comprises zinc ions coordinated by four imidazolate rings with large cavities (11.6 Å) and small pore apertures (3.4 Å) [35] which provides sensitivity to small molecule VOCs. ZIF-8 has been considered to behave as an adsorbent with molecular sieving properties. An investigation of a ZIF-8 film demonstrated the adsorption of isopropanol in a selective manner versus water [36]. A ZIF-8 based Fabry-Perot interferometer exhibited a concentration-specific reaction to a mixture of propane and nitrogen [37]. ZIF-8

film fabrication involves no substrate modification, works at room temperature and facilitates control over the thickness with one growth cycle that takes less than an hour [37,38]. In addition to being sensitive to organic vapours [36,37], ZIF-8 has been selected over other MOFs (and ZIFs) due to simplicity in fabrication and deposition of the thin film. The procedure for ZIF-8 film fabrication involves no substrate modification [37], works at room temperature and facilitates control over the thickness with one growth cycle that takes less than an hour. In addition, since ZIF-8 is hydrophobic no significant response to the relative humidity (even at relative humidity larger than 70%) is observed [39]. We have recently demonstrated for the first time, to the best of our knowledge, proof of concept data for the detection VOCs using a LPG coated with ZIF-8 [39]. A LPG based sensor coated with a ZIF-8 thin film exposed to methanol, ethanol and acetone vapours demonstrates a high sensitivity to all analytes tested, suggesting sensitivity towards low chain VOCs due to the small pore apertures (3.4 Å [35]).

However, before systems based on the technology can be widely deployed, it is essential that the sensor operates under optimized conditions in terms of both sensitivity and signal extraction. The research described here addresses these challenges. The sensitivity of the sensor is improved significantly by adjusting the grating period in such a way that the sensor operates precisely at the PMTP. This operation also facilitates the development of a novel signal processing method applied to the measured LPG spectrum. Higher sensitivity is obtained when the sensor operates in the proximity of the PMTP associated with the occurrence of two attenuation bands in the spectrum, both of them associated with the same cladding mode. The relationship between the LPG spectrum and analyte concentration is usually tracked via the change in the central wavelength associated with distinct cladding modes. When two attenuation bands are present, the shift of the individual bands can be tracked or the difference between the central wavelengths related to those attenuation bands can be used for the evaluation of the sensor performance. The latter one gives the higher sensitivity [39]. When the sensor is operating precisely at the PMTP a U-shaped band is present. In this case changes in the transmission at the central wavelength can be used for the measurement of target analytes [42]. A novel alternative proposed here is that changes in the bandwidth of the U-shaped band can also be related to the target analyte. This approach is compared with alternatives based on monitoring the intensity and central wavelength changes.

The next section presents the method of manufacture of ZIF-8 films on LPGs with 2 different periods, one in the proximity of and one precisely at the PMTP; the test methodology for the sensors; and the novel signal processing method proposed. Section 3 shows results demonstrating the performance over a wide concentration range for different VOCs. Discussions and Conclusions follow in Sections 4 and 5 respectively.

2. Methodology

2.1. Materials

Zinc nitrate hexahydrate, 2-metyl-imidazole, methanol, ethanol, 2-propanol and acetone were purchased from Sigma-Aldrich. All of the chemicals were analytical grade reagents and used without further purification.

2.2. Long period grating fabrication

LPGs with grating periods of 109.0 and 109.5 μm and length of 30 mm (further referred to as Sensor A and Sensor B, respectively) were fabricated in photosensitive boron–germanium co-doped optical fibre (Fibercore PS750) using custom made amplitude
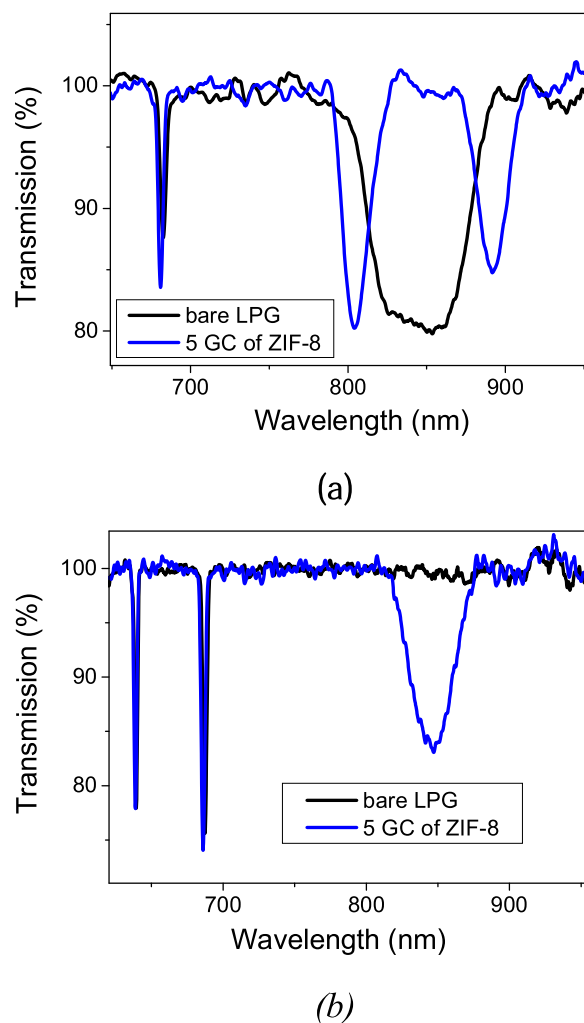

(a)

(b)

Fig. 1. Transmission spectrum of a LPG with period of a) 109.0 μm–Sensor A and b) 109.5 μm–Sensor B measured in air: uncoated (black) and coated with 5 growth cycles of ZIF-8 (blue), GC, growth cycle. Sensor A is close to the PMTP and Sensor B precisely at the PMTP. (For interpretation of the references to colour in this figure legend, the reader is referred to the web version of this article.)

masks made of 1Cr18Ni9Ti steel alloy. The grating periods of 109.0 and 109.5 μm were chosen so that the LPG operates in the proximity and exactly at the PMTP, respectively, after the deposition of the thin film of ZIF-8. The chemical sensitivity comparison performed for both sensors is further described in Section 2.4. Prior to exposure to the output from the laser, the polyacrylate jacket of the fibre was mechanically removed over the section of the proposed grating. The laser used to side-illuminate optical fibre was a frequency quadrupled Nd:YAG laser emitting at a wavelength of 266 nm (Continuum minilite I), output power of 5 mW and beam diameter 3 mm. A cylindrical lens with a focal length of 100 mm was used to focus the beam into the core of the fibre, through an amplitude mask, producing a 3 mm long line focus aligned with the axis of the fibre [40]. The use of an optical fibre with a short cut-off wavelength (∼640 nm) ensures that resonance bands at their PMTP lie towards the red end of the visible spectrum, allowing the transmission spectrum of the LPG to be monitored using an inexpensive light source, halogen lamp, and a low-cost CCD spectrometer. The transmission spectrum of the optical fibre was recorded by coupling the output from a tungsten-halogen lamp (Ocean Optics HL-2000) into the fibre and analysing the transmitted light using a fibre coupled CCD spectrometer (Ocean Optics HR4000, with the resolution of 0.22 nm).

2.3. Sensor functionalization

The LPG was coated with ZIF-8 following the process described in [37,38] and demonstrated on the surface of an optical fibre LPG in our previous work [39]. Briefly, the LPG was fixed in a custom designed holder to keep the LPG taut and straight. The LPG was placed inside a Petri dish and covered by the film forming solution (15 ml of 12.5 mM zinc nitrate hexahydrate and 15 ml of 25 mM 2-metyl-imidazole in methanol) for a period of 30 min. Then the LPG was washed by methanol and dried under nitrogen flow. The process was repeated to obtain thicker films consisting of 5 growth cycles. The transmission spectrum of the LPG was monitored during each deposition step. There was no indication that the film may be removed due to speed of the immersion as continuous building of the film was confirmed via the changes in the transmission spectrum.

2.4. Organic vapour testing

The response of the LPG to methanol, ethanol, 2-propanol and acetone was investigated with the fibre positioned in an environmental chamber composed of a closed polytetrafluoroethylene (PTFE) box (15 × 15 × 15 cm with a total volume of 3.375 l). The LPG was fixed 5 cm above the base. The chemical of interest (volume of 10 and 50 μl or 0.5 and 2 μl for experiments conducted with Sensor A and Sensor B, respectively) was injected from the top of the box by a pipette and the transmission spectrum was monitored and recorded. The concentration of the analyte was calculated according to the amount of the solution injected and the volume of the box. Sensor A was exposed to methanol, ethanol and acetone concentrations ranging from 1790 to 27900, 1240 to 24800 and 987 to 19700 ppm, respectively. Sensor B operates more closely to the PMTP and thus higher sensitivity was expected. This hypothesis was tested by exposing Sensor B to lower concentration of acetone and ethanol vapours in a range of 49–543 and 62–666 ppm, respectively. The temperature and relative humidity levels were simultaneously recorded using iButton[®] commercial data logger (iButton[®] Hygrochron Temperature/Humidity Logger DS1923, Maxim Integrated[TM]). The temperature level was stable during the experiments with minor fluctuations up to 0.5 °C. All experiments have been conducted in a temperature and humidity controlled laboratory.

2.5. Signal processing

As described in Section 1, three methods for the evaluation of the changes in the LPG transmission spectrum are compared in this paper: via i) changes in the central wavelength difference, ii) changes in the transmission at the central wavelength of the U-shaped attenuation band and iii) changes in the bandwidth of the U-shaped attenuation band.
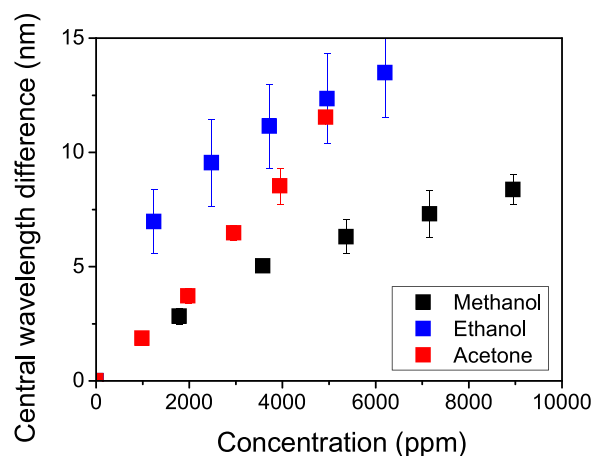
LODs have been calculated using the following equation

$$LOD = \frac{S_d}{m} \tag{2}$$

where *LOD* indicates limit of detection, S_d is the average standard deviation obtained over the values measured in stable conditions (at each concentration level) over the 2 min period and *m* is the slope of the calibration curve (a linear approximation was used for the range up to 10,000 ppm).
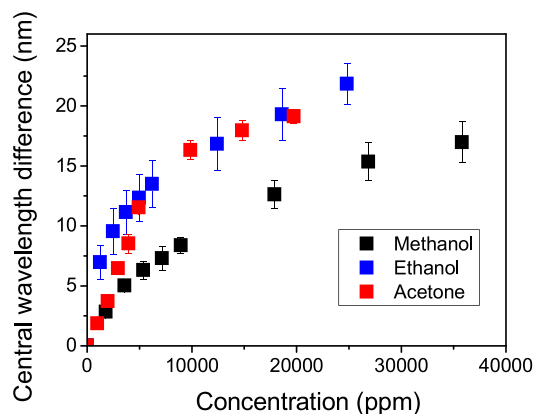
(a)

(b)

Fig. 2. Sensor A: calibration curves for methanol (black), ethanol (blue) and acetone (red). Error bars represent the standard deviation of the values taken over the three separate experiments b) shows the inset of a) where the data up to 10,000 ppm are shown for clarity. (For interpretation of the references to colour in this figure legend, the reader is referred to the web version of this article.)

3. Results

3.1. Sensor fabrication

[Fig. 1](#)a shows the transmission spectra of a bare LPG and a LPG coated with 5 layers of ZIF-8 for a grating period of 109.0 μm (Sensor A). The "U" shaped band of the LP_{019} cladding mode splits into two attenuation bands after the deposition of the film. [Fig. 1](#)b shows a grating period of 109.5 μm, where no attenuation band corresponding to the LP_{019} cladding mode is observed before the coating process and which is developed only after the deposition of ZIF-8 (Sensor B). As discussed in Section 2.2, this is precisely at the PMTP and is likely to result in the highest sensitivity.

3.2. Sensor A: volatile organic compounds sensing

Sensor A was calibrated via three repeated measurements and its performance was evaluated via the change in central wavelengths difference method described in Section 2.5. Without the presence of the U-shaped attenuation band, the other 2 signal processing methods described in Section 2.5 cannot be applied ([Fig. 1](#)a, blue line). The sensitivity to ethanol and acetone was observed to be higher than for methanol, [Fig. 2](#). At low concentrations and up

to 5000 ppm, the sensor shows the highest sensitivity to ethanol, inducing a central wavelength shift of 12.34 ± 1.97 nm at 4963 ppm.

Higher sensitivity to all tested analytes was observed in comparison to the results presented in [39] measured using the central wavelengths difference corresponding to the LPG coated with 5 growth cycles of ZIF-8. For example, the change in the central wavelength difference induced by ~9000 ppm of methanol vapour was measured to be 8.37 nm in comparison to 2.17 nm obtained in our preliminary work [39]. The higher sensitivity of the current sensors is due to the smaller separation of the attenuation bands in air as the sensor operates closer to the PMTP.

The differences in the sensitivity can be associated with the size of the molecule, where the smaller methanol molecules have lower capture rate in the cavities at lower concentrations. The functional group can also play a role and can explain the bigger response of the sensor to ethanol in comparison to acetone at low levels up to 5000 ppm. The shape of the curve indicates the saturation of the sensor at high concentrations over 20,000 ppm. For simplicity, a linear approximation is assumed in the range up to 10,000 ppm in order to calculate the LOD using Eq. [2]. LODs of 164.4, 421.7 and 162.8 ppm were obtained for acetone, methanol and ethanol respectively using the data presented in Fig. 2.

3.3. Sensor B: volatile organic compounds sensing

The high sensitivity of Sensor A to ethanol and acetone vapours leads to the further investigation of improving the LOD by operating the LPG precisely at the PMTP using a grating period of 109.5 μm. As described in Section 2.4, as higher sensitivity was anticipated, lower concentrations of ethanol and acetone (62–666 and 49–543 ppm, respectively) were used. Due to the presence of the U-shaped band (Fig. 2b, blue line) it is now possible to track changes in the spectrum due to a change in the transmission at the central wavelength and also the change in bandwidth of the attenuation band. Due to the absence of the dual attenuation bands, it is not possible to use the central wavelength difference method used in Section 3.2.

The performance of Sensor B has been evaluated via the changes in transmission at the central wavelength. For instance, concentration of 543 ppm of acetone vapour induced a change of approximately 2% in transmission at the central wavelength of Sensor B, Fig. S1a. Similarly, a concentration of 666 ppm of ethanol caused approximately 3% change in transmission, Fig. S1b. The response of Sensor B to acetone vapours in a range from 49 to 543 ppm based on the changes in the transmission at the central

wavelength are shown in Fig. 3a. Similarly, the response of Sensor B to ethanol vapours in range from 62 to 666 ppm is shown in Fig. 2b. These values were used to calculate the standard the standard deviation of the intensity changes 10 mV and for this reason the adequate change of 0.1% in transmission has been used for the calculation of the LOD. LODs of 25.64 and 21.28 ppm have been calculated for acetone and ethanol respectively for Sensor B based on the change in transmission at the central wavelength of the attenuation band corresponding to LP_{019} cladding mode.

As described in Section 2.5, the change in the bandwidth of the U-shaped band represents a novel approach for the evaluation of LPG based sensors. Tracking the width of the attenuation band overcomes any intensity based issues as there is no need to track the absolute intensity at reference wavelength. The evolution of the differences in the width of the attenuation band corresponding to LP_{019} cladding mode has been demonstrated in response to ethanol vapours in the range of 62–666 ppm, Fig. 4a. The bandwidth was measured at the wavelengths corresponding to 85% of transmission, as shown in detail for the left section of the attenuation band (in the region of 820 nm) in Fig. 4b. As an example, the bandwidth increased from 54.68 to 66.27 nm in response to 666 ppm of ethanol, Fig. 4.

The calibration curves (Fig. 5) were calculated based on the change of bandwidth via the results of three repeated measurements. The slope of 0.018 ± 0.0015 nm/ppm was obtained for ethanol, Fig. 5. The error bar represents the standard deviation of the calculated slope value. Similarly, the response of Sensor B has been evaluated for acetone over the range of 49–543 ppm with a slope of width difference of 0.015 ± 0.001 nm/ppm. The LOD of the sensor has been calculated in relation to a standard deviation of 0.1 nm and following Eq. (2). LOD of 5.56 and 6.67 ppm was obtained for ethanol and acetone, respectively. The sensor's performance and dynamic change in time can also be tracked via the shift of the central wavelength of the LP_{018} cladding mode. As an example, Sensor B responded even to the lowest concentration of 61 ppm of ethanol and showed a further shift of the central wavelength up to highest concentration of 666 ppm of ethanol, inducing the shift of the central wavelength of 0.60 nm at 666 ppm, Fig. S2.

4. Discussion

The sensitivity of Sensor A and Sensor B using different data evaluation techniques over the range of analytes is compared in Table 2. The obtained sensitivity for the ethanol vapour measure-
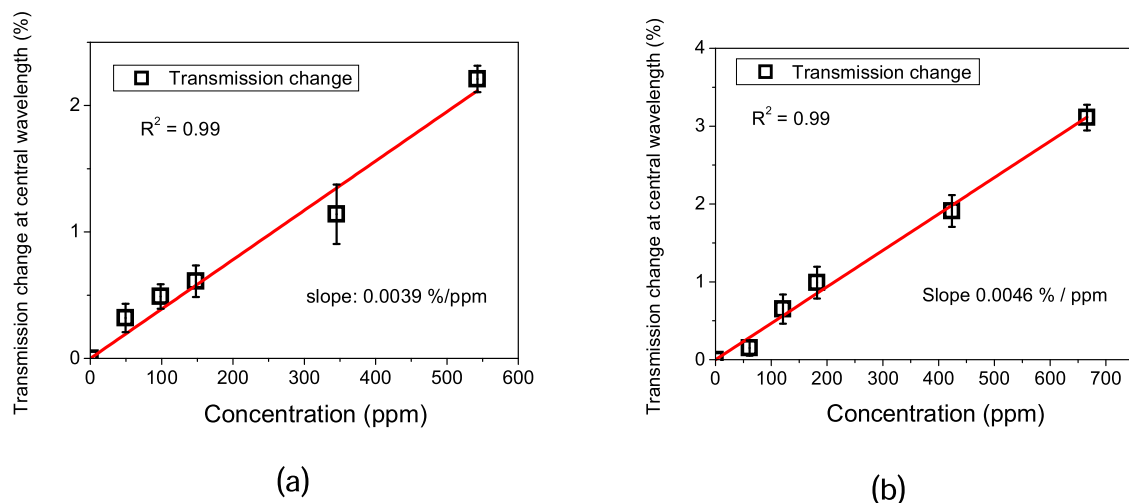

Fig. 3. Sensor B: calibration curve based on the change in transmission loss (the error bars represented by the standard deviation of the value at the stable conditions at each concentration step are smaller than the data points) a) acetone and b) ethanol.

Table 2
Comparison of the performance of Sensor A and Sensor B towards organic vapours across the different evaluation techniques.

Sensor	Analyte	Conc. range [ppm]	Data evaluation technique	Sensitivity [nm/1000 ppm]	LOD [ppm]
Sensor A	MetOH	1790 to 27,900	CW shift	0.83 ± 0.08	421.7
Sensor A	EtOH	1240 to 24,800	CW shift	2.58 ± 0.28	162.8
Sensor A	Acetone	987 to 19,700	CW shift	1.46 ± 0.06	164.4
Sensor B	EtOH	61 to 666	$\triangle$ Bandwidth	18 ± 1.5	5.56
Sensor B	EtOH	61 to 666	$\triangle$ Transmission	$4.5 \pm 0.2^{**}$	21.28
Sensor B	Acetone	49 to 543	$\triangle$ Bandwidth	15 ± 1	6.67
Sensor B	Acetone	49 to 543	$\triangle$ Transmission	$3.9 \pm 0.2^{**}$	25.64

* The linear response approximation was assumed for the sensitivity calculation.
** The units are transmission percent loss per 1000 ppm.
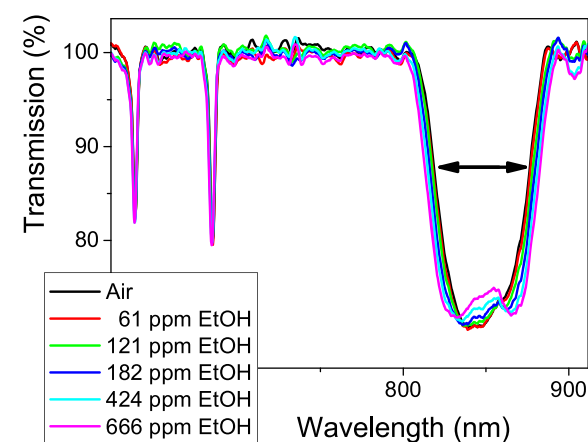
(a)
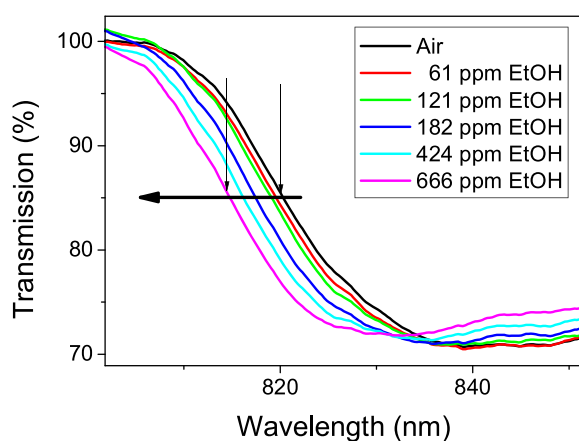
(b)

Fig. 4. Sensor B: a) Transmission spectra and b) left section of the attenuation band corresponding to LP_{019} cladding mode in detail, measured in air (black), in response to 62 (red), 121 (green), 181 (blue), 424 (cyan) and 666 ppm of ethanol (magenta). (For interpretation of the references to colour in this figure legend, the reader is referred to the web version of this article.)

ment fulfils the criteria for ethanol limit values for drivers in the range of 0.2–0.8% in blood (the values differ across the countries. The conversion of those limits into the amount of ethanol in gas phase will give the range of 30–130 ppm [2].

The obtained sensitivity for the detection of acetone is sufficient to monitor occupational exposure in the workplace. The Health and Safety Executive in the UK states the exposure limits of 500 and 1500 ppm of acetone as a weighted average over 8 h and 15 min respectively [43]. Electrochemical based sensor represent the com-

peting developing technology in a field of new acetone gas sensors, the LODs vary from 0.4 to 500 ppm, however, they suffer from high operating temperature (200–500 °C) and sometimes were tested only in N_2 atmosphere [44]. The concentration ranges from 1.7 ppm to 3.7 ppm could be detected in breath of people with diagnosed diabetic conditions in comparison to 0.8 ppm measured in breath of healthy people [3]. Furthermore, the LPG based sensors with current design can be used for measurement of acetone in breath for the monitoring of ketogenic diet and associated weight loss (range of 2–40 ppm) or diabetic ketoacidosis (75–1250 ppm) [4].

The obtained LOD in a range of units of ppm for ethanol and acetone suggests the potential of the sensor for real world applications. Further improvement could be made by using a higher resolution spectrometer in combination with a new approach of data analysis (including the transmission, central wavelength and width change). The sub ppm level will be highly desired in health monitoring applications, e.g. breath analysis. The higher sensitivity could be also achieved using the thicker film and this hypothesis should be tested in future work. Although there is a clear cross sensitivity to different VOCs many of the tests can be designed to reduce this problem. It is expected however that one concentration will be significantly higher than the others for many applications. For example, in breath tests for alcohol consumption, ethanol levels will be two orders of magnitude higher in breath (when they reach the levels that break the law) in comparison to the other VOCs present in the breath. Similarly, patients suffering from ketoacidosis are expected to have much higher concentration of acetone in their breath in comparison to other VOCs. The implementation of the sensor into an array will enable in-situ measurement, e.g. for the occupational exposure, or any industrial monitoring, where a reference grating is necessary to subtract any temperature effect [45]. The cross-sensitivity to water vapour in highly humid environment should also be included to test the possibility of using this sensor in breath analysis [46].

5. Conclusions

ZIF-8 films with controllable thickness have been deposited successfully onto the surface of an optical fibre LPG and the response of the transmission spectra has been characterized for different volatile organic compounds (ethanol, acetone and methanol). The importance of precisely setting the grating period so that the long period grating sensor operates exactly at the phase matching turning point has also been demonstrated. Furthermore three different signal processing methods for monitoring the change of the transmission spectra have been evaluated. The highest sensitivity has been obtained when the LPG operates precisely at the phase matching turning point and the bandwidth of the U-shaped attenuation band is measured. For example for ethanol this optimisation process results in the calculated limit of detection reducing from 163 ppm to 5.6 ppm.
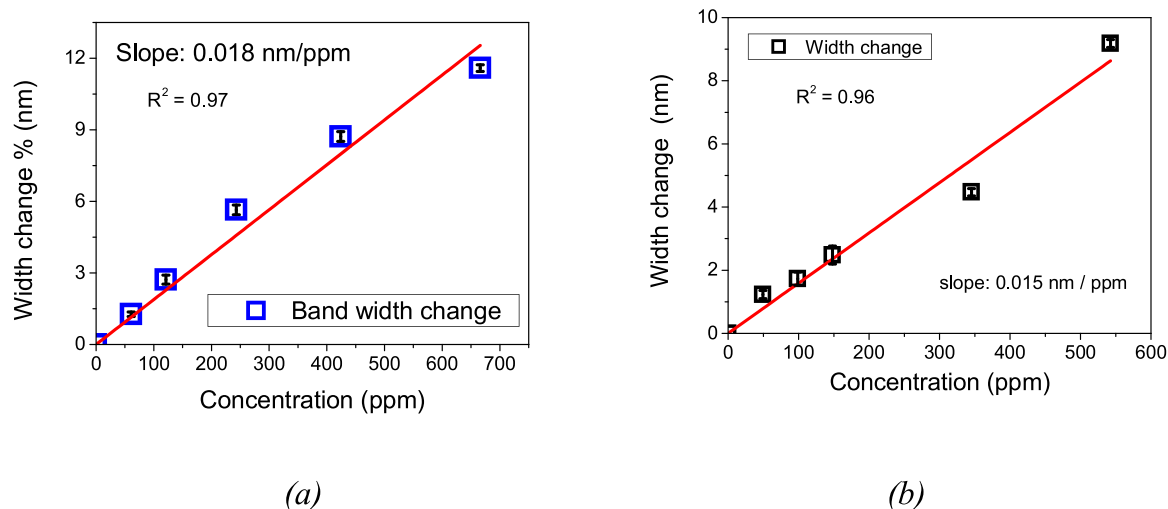
Fig. 5. Sensor B: a) acetone and b) ethanol calibration curve based on the changes in band width (the error bars represented by the standard deviation of the value at the stable conditions at each concentration step are smaller than the data points).

Acknowledgment

References

[1] E. Wongrat, N. Chanlek, C. Chueaiarrom, B. Samransuksamer, N. Hongsith, S. Choopun, Low temperature ethanol response enhancement of ZnO nanostructures sensor decorated with gold nanoparticles exposed to UV illumination, Sens. Actuators A Phys. 251 (2016) 188–197, http://dx.doi.org/10.1016/j.sna.2016.10.022 ([Internet] Available from).

[2] G. Domènech-Gil, J. Samà, P. Pellegrino, S. Barth, I. Gràcia, C. Cané, et al., Gas nanosensors based on individual indium oxide nanostructures, Procedia Eng. 120 (2015) 795–798, http://dx.doi.org/10.1016/j.snb.2016.07.084 ([Internet] Available from).

[3] C. Deng, J. Zhang, X. Yu, W. Zhang, X. Zhang, Determination of acetone in human breath by gas chromatography-mass spectrometry and solid-phase microextraction with on-fiber derivatization, J. Chromatogr. B Anal. Technol. Biomed. Life Sci. 810 (2) (2004) 269–275.

[4] J.C. Anderson, Measuring breath acetone for monitoring fat loss: review, Obesity 23 (12) (2015) 2327–2334.

[5] Federal-provincial advisory committe on environmental and occupational health, in: Indoor Air Quality in Office Buildings: A Technical Guide, 1995, pp. 1–57.

[6] M. Parthibavarman, B. Renganathan, D. Sastikumar, Development of high sensitivity ethanol gas sensor based on Co-doped SnO2 nanoparticles by microwave irradiation technique, Curr. Appl. Phys. 13 (7) (2013) 1537–1544, http://dx.doi.org/10.1016/j.cap.2013.05.016 ([Internet] Available from).

[7] M.Z. Ahmad, A.Z. Sadek, J.Z. Ou, M.H. Yaacob, K. Latham, W. Wlodarski, Facile synthesis of nanostructured WO3 thin films and their characterization for ethanol sensing, Mater. Chem. Phys. 141 (2-3) (2013) 912–919, http://dx.doi.org/10.1016/j.matchemphys.2013.06.022 ([Internet] Available from).

[8] H. Ko, S. Park, S. An, C. Lee, Enhanced ethanol sensing properties of TiO2/ZnO core-shell nanorod sensors, Curr. Appl. Phys. 13 (2013) 919–924, http://dx.doi.org/10.1016/j.cap.2013.01.020 ([Internet] Available from).

[9] L. Wang, T. Fei, Z. Lou, T. Zhang, Three-dimensional hierarchical flowerlike α-Fe 2 O 3 nanostructures: synthesis and ethanol-sensing properties, Appl Mater Interfaces. (2011) 4689–9694.

[10] E. Wongrat, P. Pimpang, S. Choopun, Comparative study of ethanol sensor based on gold nanoparticles: ZnO nanostructure and gold: ZnO nanostructure, Appl. Surf. Sci. 256 (4) (2009) 968–971.

[11] L.R. Shobin, B. Renganathan, D. Sastikumar, K.C. Park, S. Manivannan, Pure and iso-butyl methyl ketone treated multi-walled carbon nanotubes for ethanol and methanol vapor sensing, IEEE Sens. J. 14 (4) (2014) 1238–1243.

[12] M. NaderiNasrabadi, Y. Mortazavi, A.A. Khodadadi, Highly sensitive and selective Gd2O3-doped SnO2 ethanol sensors synthesized by a high temperature and pressure solvothermal method in a microreactor, Sens. Actuators B Chem. 230 (2016) 130–139, http://dx.doi.org/10.1016/j.snb.2016.02.045 ([Internet] Available from).

[13] A.D. Kersey, A review of recent developments in fiber optic sensor technology, Opt. Fiber Technol. 2 (1996) 291–317 ([Internet] Available from http://www.sciencedirect.com/science/article/pii/S106852009690036X).

[14] A. Cusano, M. Consales, A. Crescitelli, M. Penza, P. Aversa, P.D. Veneri, et al., Charge transfer effects on the sensing properties of fiber optic chemical nano-sensors based on single-walled carbon nanotubes, Carbon N. Y. 47 (3) (2009) 782–788, http://dx.doi.org/10.1016/j.carbon.2008.11.014 ([Internet] Available from).

[15] C. Elosúa, C. Bariáin, I.R. Matías, F.J. Arregui, A. Luquin, E. Vergara, et al., Indicator immobilization on Fabry-Perot nanocavities towards development of fiber optic sensors, Sens. Actuators B Chem. 130 (1) (2008) 158–163.

[16] S.C. Terrones, C.E. Aguado, C. Bariáin, A.S. Carretero, I.R. Matíías Maestro, A.F. Gutieírrez, et al., Volatile-organic-compound optic fiber sensor using a gold-silver vapochromic complex, Opt. Eng. 45 (4) (2006) 44401.

[17] Z.H. Zhang, R. Lockwood, J.G.C. Veinot, A. Meldrum, Detection of ethanol and water vapor with silicon quantum dots coupled to an optical fiber, Sens. Actuators B Chem. 181 (2013) 523–528, http://dx.doi.org/10.1016/j.snb.2013.01.070 ([Internet] Available from).

[18] M.Q. Lokman, H.R. Bin Abdul Rahim, S.W. Harun, G.L. Hornyak, W.S. Mohammed, Light backscattering (e.g. reflectance) by ZnO nanorods on tips of plastic optical fibres with application for humidity and alcohol vapour sensing, Micro. Nano Lett. 11 (12) (2016) 832–836 ([Internet] Available from http://digital-library.theiet.org/content/journals/10.1049/mnl.2016.0321).

[19] S. Manivannan, A.M. Saranya, B. Renganathan, D. Sastikumar, G. Gobi, K.C. Park, Single-walled carbon nanotubes wrapped poly-methyl methacrylate fiber optic sensor for ammonia, ethanol and methanol vapors at room temperature, Sens. Actuators B Chem. 171–172 (2012) 634–638, http://dx.doi.org/10.1016/j.snb.2012.05.045 ([Internet] Available from).

[20] B. Renganathan, D. Sastikumar, R. Srinivasan, A.R. Ganesan, Nanocrystalline samarium oxide coated fiber optic gas sensor, Mater. Sci. Eng. B Solid-State Mater. Adv. Technol. 186 (1) (2014) 122–127, http://dx.doi.org/10.1016/j.mseb.2014.03.018 ([Internet] Available from).

[21] T. Kavinkumar, D. Sastikumar, S. Manivannan, Effect of functional groups on dielectric, optical gas sensing properties of graphene oxide and reduced graphene oxide at room temperature, RSC Adv. 5 (14) (2015) 10816–10825 ([Internet] Available from) http://xlink.rsc.org/?DOI=C4RA12766H.

[22] S. Sharifpour-Boushehri, S.M. Hosseini-Golgoo, M.H. Sheikhi, A low cost and reliable fiber optic ethanol sensor based on nano-sized SnO2, Opt. Fiber Technol. 24 (2015) 93–99, http://dx.doi.org/10.1016/j.yofte.2015.05.002 ([Internet] Available from).

[23] Y. Ko, H. Tsai, K. Lin, Y. Chen, H. Yang, Reusable macroporous photonic crystal-based ethanol vapor detectors by doctor blade coating, J. Colloid Interface Sci. 487 (2017) 360–369, http://dx.doi.org/10.1016/j.jcis.2016.10.061 ([Internet] Available from).

[24] M. Konstantaki, A. Klini, D. Anglos, S. Pissadakis, An ethanol vapor detection probe based on a ZnO nanorod coated optical fiber long period grating, Opt. Express 20 (8) (2012) 8472.

[25] H. Kudo, M. Sawai, Y. Suzuki, X. Wang, T. Gessei, D. Takahashi, et al., Fiber-optic bio-sniffer (biochemical gas sensor) for high-selective monitoring of ethanol vapor using 335 nm UV-LED, Sens. Actuators B Chem. 147 (2) (2010) 676–680, http://dx.doi.org/10.1016/j.snb.2010.03.066 ([Internet] Available from).

[26] A. Bearzotti, A. Macagnano, P. Papa, I. Venditti, E. Zampetti, A study of a QCM sensor based on pentacene for the detection of BTX vapors in air, Sens. Actuators B Chem. 240 (2017) 1160–1164, http://dx.doi.org/10.1016/j.snb.2016.09.097 ([Internet] Available from).

[27] G. Rego, A review of refractometric sensors based on long period fibre gratings, Sci. World J. 2013 (2013).

[28] S.W. James, R.P. Tatam, Optical fibre long-period grating sensors: characteristics and application, Meas. Sci. Technol. 14 (5) (2003) R49–61.

[29] S.M. Topliss, S.W. James, F. Davis, S.P.J. Higson, R.P. Tatam, Optical fibre long period grating based selective vapour sensing of volatile organic compounds, Sens. Actuators B Chem. 143 (2) (2010) 629–634.
[30] X. Shu, L. Zhang, I. Bennion, Sensitivity characteristics of long-period fiber gratings, J. Light Technol. 20 (2) (2002) 255–266.
[31] H.J. Patrick, A.D. Kersey, F. Bucholtz, Analysis of the response of long period fiber gratings to external index of refraction, J. Light Technol. 16 (9) (1998) 1606–1612.
[32] P. Kumar, A. Deep, K.-H. Kim, Metal organic frameworks for sensing applications, TrAC Trends Anal. Chem. 73 (2015) 39–53 ([Internet] Available from http://www.sciencedirect.com/science/article/pii/S0165993615001090).
[33] L.E. Kreno, K. Leong, O.K. Farha, M. Allendorf, R.P. Van Duyne, J.T. Hupp, Metal À Organic Framework Materials as Chemical Sensors, Chem. Rev. 112 (2012) 1105–1125.
[34] A. Betard, R.A. Fischer, Metal À Organic Framework Thin Films: From Fundamentals to, 2012, pp. 1055–1083.
[35] K.S. Park, Z. Ni, A.P. Côté, J.Y. Choi, R. Huang, F.J. Uribe-Romo, et al., Exceptional chemical and thermal stability of zeolitic imidazolate frameworks, Proc. Natl. Acad. Sci. U. S. A. 103 (27) (2006) 10186–10191.
[36] A. Demessence, C. Boissière, D. Grosso, P. Horcajada, C. Serre, G. Férey, et al., Adsorption properties in high optical quality nanoZIF-8 thin films with tunable thickness, J. Mater. Chem. 20 (36) (2010) 7676.
[37] G. Lu, J.T. Hupp, Metal Organic Franeworks as Sensors A ZIF (Based Fabry Perot Device as a Selective Sensor for Chemical Vapours and Gases.pdf, 2010, pp. 7832–7833.
[38] G. Lu, O.K. Farha, W. Zhang, F. Huo, J.T. Hupp, Engineering ZIF-8 thin films for hybrid MOF-based devices, Adv. Mater. 24 (2012) 3970–3974.
[39] J. Hromadka, B. Tokay, S. James, R.P. Tatam, S. Korposh, Optical fibre long period grating gas sensor modified with metal organic framework thin films, Sens. Actuators B Chem. 221 (2015) 891–899.
[40] J. Hromadka, R. Correia, S. Korposh, Fabrication of fiber optic long period gratings operating at the phase matching turning point using an amplitude mask, Proceedings of SPIE–The International Society for Optical Engineering (2016).
[42] S. Korposh, R. Selyanchyn, W. Yasukochi, S.W. Lee, S.W. James, R.P. Tatam, Optical fibre long period grating with a nanoporous coating formed from silica nanoparticles for ammonia sensing in water, Mater. Chem. Phys. 133 (2-3) (2012) 784–792, http://dx.doi.org/10.1016/j.matchemphys.2012.01.094 ([Internet] Available from).
[43] EH4O/2005 Workplace Exposure Limits EH4O/2005 Workplace Exposure Limits. Eh40/2005, Health and Safety Executive, 2011, pp. 1–74 (March 2013).
[44] K.W. Kao, M.C. Hsu, Y.H. Chang, S. Gwo, J. Andrew Yeh, A Sub-ppm acetone gas sensor for diabetes detection using 10 nm thick ultrathin InN FETs, Sens. (Switzerland) 12 (6) (2012) 7157–7168.
[45] J. Hromadka, S. Korposh, M.C. Partridge, S.W. James, F. Davis, D. Crump, et al., Multi-parameter measurements using optical fibre long period gratings for indoor air quality monitoring, Sens.Actuators B Chem. 244 (2017).
[46] F.U. Hernandez, S.P. Morgan, B.R. Hayes-gill, D. Harvey, W. Kinnear, A. Norris, et al., Characterization and use of a fiber optic sensor based on PAH/SiO 2 film for humidity sensing in ventilator care equipment, IEEE Trans. Biomed. Eng. 63 (9) (2016) 1985–1992.

Biographies

Dr. Jiri Hromadka received both his bachelor and master degrees in 2011 and 2013 respectively in environmental sciences from Charles University in Prague (Czech Republic) and an MSc in Health and the Environment from Cranfield University in 2013 and Ph.D. degree from the University of Nottingham in 2017. His research focuses on a development of fibre optic chemical sensors with a special interest in environmental applications.

Dr Begum Tokay received her bachelor (1999) and master (2001) degrees in Chemical Engineering from Istanbul Technical University (ITU), Istanbul (Turkey). She was awarded a PhD in Chemical Engineering (ITU, 2007) for work on nanosize zeolite crystallization and growth mechanism during synthesis from clear solutions. She worked atthe University of Colorado, Boulder (USA) as a research associate on development of zeolite membranes for separations of gas, liquid or vapour mixtures in the Department of Chemical and Biological Engineering from 2008 to 2011. She worked as a lecturer at the Middle East Technical University (Northern Cyprus Campus) in the Chemical Engineering Program from 2011 to 2012. She is currently assistant professor at the University of Nottingham. Her research interests focus on application and development of membranes, thin films and microporous & mesoporous materials

Dr Ricardo Goncalves Correia graduated in 2004 with a 5 year degree in Instrumentation and Industrial Quality Engineering from the Superior Institute of Engineering of Porto. In 2005 he joined the Engineering Photonics group at Cranfield University to pursuit a PhD in the development of a fibre optic pore pressure sensor employing Fibre Bragg Gratings. As a post-doctoral fellow he has further developed interferometric and Bragg grating based fibre optic sensors for civil and aerospace engineering applications. In 2015 he joined the UoN where he is currently working on the development of fibre optic sensors for healthcare applications.

Professor Stephen P. Morgan is Professor of Biomedical Engineering at UoN. Since 1992, he has investigated novel optical techniques for imaging and spectroscopy of tissue using laser Doppler flowmeter y, acousto-optic imaging and hyperspectral imaging. His research involves the development of devices to monitor the microcirculation specifically in tissue breakdown and wound healing. For example, he currently developing a novel endotracheal tube that can monitor the microcirculation at the cuff/trachea interface. Recent work involves the integration of optical fibre sensors into textiles. These sensing systems, incorporated into garments can monitor pressure, temperature and the microcirculation.

Dr Serhiy Korposh received both his bachelor and master degrees in 2001 and 2002 respectively in physics from Uzhgorod National University, Transcarpathia (Ukraine) and Ph.D. degree from Cranfield University in 2007. He worked as a post-doctoral researcher on development of the novel materials for chemical sensors in the Graduate School of Environmental Engineering of the University of Kitakyushu from 2008 to 2012. From 2012–2013 he worked as a research fellow in the Department of Engineering Photonics, Cranfield University. He is currently Lecturer at the University of Nottingham. His research interest lies in the field of application and development of fibre-optic chemical sensors modified with the sensitive materials.